Covalently Crosslinked Graphene Oxide Membranes by Esterification Reactions for Ions Separation

Zhiqian Jia, [*] Yan Wang

We present a method to prepare covalently crosslinked graphene oxide (GO) membranes with adjustable intersheet spacing by esterification reactions, using dicarboxylic acids, diols or polyols as the crosslinkers and hydrochloric acid as the catalyst. For dicarboxylic acids, with the increased length of molecular chain, the intersheet spacing, elastic moduli and permeation fluxes of GO membranes generally increase. The elastic modulus of hexanedioidc acid crosslinked membrane is 15.6 times that of the pristine one, and the selectivity of K^+/Mg^{2+} attains to 6.1. There exists an optimum chain length of crosslinkers. For diols or polyols, the hydrophobic substituents ($-CH_3$) tend to enlarge the intersheet spacing of GO membranes, while the hydrophilic substituents ($-OH$) favor the penetration of hydrated ions. The elastic moduli, permeation fluxes and selectivity of diols or polyols crosslinked membranes are relatively lower than those of dicarboxylic acids crosslinked ones.

[*] *Lab for Membrane Science and Technology, College of Chemistry, Beijing Normal University, Beijing 100875, China. Email:zhqjia@bnu.edu.cn*

Introduction

Membrane processes, such as Nanofiltration, ultrafiltration and forward osmosis, are among the most effective strategies to achieve high removal of contaminants from water. However, traditional membranes still face important technical limits, such as chlorine resistance, fouling resistance, and control of thickness and pores size distribution.[1] Graphene oxide (GO), which is prepared by the chemical exfoliation of graphite using strong oxidants such as $KMnO_4$ dissolved in concentrated H_2SO_4,[2, 3] has been demonstrated to be another type of promising membrane material due to its ease of synthesis and scale-up. GO sheets can be reassembled into large-area membranes with interlocked structure and controlled thickness by drop-casting, spin-coating,[4] vacuum filtration,[5] interfacial self-assembly,[6] L-B,[7] chemical vapor deposition,[8] *etc*. GO contains hydroxyl and epoxy functional groups on the basal planes, in addition to carbonyl and carboxyl groups located at the sheet edges.[9] The oxygen-containing functional groups maintain a relatively large intersheet distance and empty spaces between nonoxidized regions, resulting in the formation of a network of nanocapillaries within the GO membranes.[10, 11] Water is allowed to permeate through these nanocapillaries smoothly while other liquids, gases and vapors are blocked.[12, 13] GO membrane is considered as promising candidates in many applications such as water purification[14, 15] and gas separation[16,17].

Nevertheless, GO membranes are extremely hydrophilic, leading to its unstability in water.[18] The weak interaction between GO sheets also results in low mechanical strength of membranes.[19] To resolve these problems, chemical bonding can be created between GO sheets to prevent their dispersion in water and to enhance the mechanical properties.[20] Chemical crosslinking of GO sheets using divalent metal ions,[21] borate,[22] polyallylamine[23], polyetheramine[24], dopamine,[25] or epoxy-functionalized polyhedral oligomeric silsesquioxane,[26] produces stable and mechanically improved membranes.[27] Taking into account of the bond strength, covalent crosslinking is more preferred.

In terms of transportation through GO membranes, the control of nanocapillaries structure (e.g. intersheet spacing) or modulating the ion migration process by external field[28, 29] (e.g. electric and/or magnetic field) is of crucial importance. Herein, we prepared covalently crosslinked GO membranes by esterification reactions, using dicarboxylic acids, diols or polyols as the crosslinkers and hydrochloric acid as the catalyst. By altering the chain length, functional groups and substituents of the crosslinkers, the intersheet spacing, elastic moduli and permeation of GO membranes can be adjusted, which is potential for precise separation of ions and molecules. To our best knowledge, there has not report about GO membranes with adjustable intersheet spacing and permeation performance.

Experimentals

Materials

The chemicals, including H_2SO_4 (>98.0%), H_2O_2 (30%), hydrochloric acid (37%), $KMnO_4$, $NaNO_3$, oxalic acid (OA), propandioic acid (PA), succinic acid (SA)，hexanedioidc acid (HA), octanedioic acid (OcA), ethylene glycol (EG), 1,2-propylene glycol (PG), butylene glycol (BG), 1, 6-hexylene glycol (HG), neopentyl glycol (NPG), glycerol (GL), pentaerythritol (PER), glycerol, $K_4[Fe(CN)_6]$, $MgCl_2$, KCl, $CaCl_2$ and $NiCl_2$, were analytical grade and provided by the Beijing Chemical Factory. Graphite was bought from the Tianjin Bodi Chemical Co., Ltd. Polypropylene (PP) microfiltration membranes (pores size of 0.45 μm, diameter of 25 mm) and syringe filters were provided by Taoyuan Medical Chemical Instrument Factory, Haining, China.

Preparation of GO dispersion

The modified Hummers' method was employed for the preparation of GO powder.[30, 31] Graphite (10 g, rinsed with hydrochloric acid) was added gradually into H_2SO_4 (230 mL, containing 5 g of $NaNO_3$) maintaining below 5 °C. Subsequently, $KMnO_4$ (30 g) was added into the mixture under stirring and cooling. The system was further stirred at 35 °C for 35 min, and distilled water (460 mL) was added. The temperature was then elevated to 98°C for 15 min. The reaction was terminated by adding a large amount of distilled water (50~60 ℃, 1.4 L) and H_2O_2 (30%, 100 mL), after which the colour of the mixture became bright yellow. The mixture was filtered and washed with hydrochloric acid (5%, 2 L) to remove SO_4^{2-} ions. The filtrate was further washed with distilled water until the pH value became neutral. Exfoliation of graphite oxide was achieved by adding distilled water into GO viscous suspensions followed by ultrasonic dispersion (KX-1740QTD, 120 W) for 1 hour.

Fabrication of GO membrane

First, a certain volume of crosslinker solution was added into 0.9 mL of GO colloidal suspension (9.5 mg ml^{-1}). After ultrasonic dispersion, the mixture was filtered with a PP microfiltration membrane to obtain GO membrane. Then 0.2 mL of hydrochloric acid (9.60 mol L^{-1}) was filtered through the GO membrane. Following 0.3 mL of the hydrochloric acid was added onto the membrane, and they were kept at 80℃ for 30 min to catalyze the esterification reaction. Lastly, the membrane was washed with deionized water to remove excess hydrochloric acid and crosslinkers, and dried at room temperature.

Characterization

The FT-IR spectra of GO membranes were measured with a Nicolet 380 FT-IR spectrometer (USA). The membrane was sputtered with platinum and the morphology was observed by cold-field scanned electron microscopy (SEM S-4800, Japan). The XRD patterns were collected using Shimadzu XRD-6000 (monochromatized Cu *Kα* incident radiation). Prior to the XRD measurement, the GO membranes were kept in a desiccator overnight to attain the same humidity. The mechanical properties were tested by a universal mechanical esting machine (INSTRON-3366, USA) with stretching speed of 100%/min. X-ray photoelectron spectroscopy was analyzed using a Thermofisher ESCaLab 250Xi spectrometer.

Penetration experiments were conducted using a home-made U-tube divided by the GO membrane (diameter of 13.0 mm, thickness of 17.1 μm) into two compartments referred to as feed and permeate (Fig. 1). For penetration of single solution, the feed compartment contained KCl, $K_4Fe(CN)_6$ or glycerol aqueous

solution, respectively. For penetration of mixed solutions, the feed compartment contained the mixed $MgCl_2$, KCl, $CaCl_2$ and $NiCl_2$ aqueous solutions with the same concentration (0.050, 0.10 or 0.20 mol L^{-1}). The permeate compartment contained pure water. Both compartments were stirred magnetically to promote mass-transfer. The cations concentration in the permeate compartment was measured by ICP-AES (iCAP 6000 SERIES, Thermo Scientific) while the glycerol concentration was measured instead by a refractormeter (WYA-2WAJ, Shanghai Jingke).
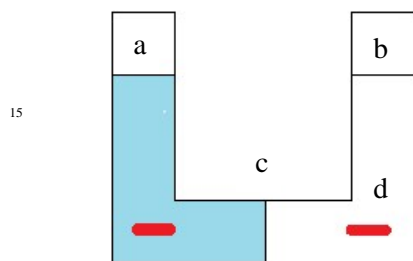

Fig.1 Diagram of U-tube for penetration experiments. (a) Feed compartment (b) Permeate compartment (c) GO membrane (d) Stir.

Results and discussions

Effects of dicarboxylic acid

0.01 mol L^{-1} of oxalic acid (OA), propandioic acid (PA), succinic acid (SA)，hexanedioidc acid (HA) and octanedioic acid (OcA) were respectively employed to crosslink the hydroxyl groups on the basal planes of GO sheets. After ultrasonic mixing of crosslinker with GO colloidal suspension, the mixture was filtered with PP porous membranes. Then hydrochloric acid was added and the esterification reaction was conducted at 80℃ for 30 min. Scheme 1 shows the schematic of the crosslinking mechanism. The hydroxyl groups on the adjacent GO sheets react with the carboxyl of dicarboxylic acid and form covalent bonds between the GO sheets.
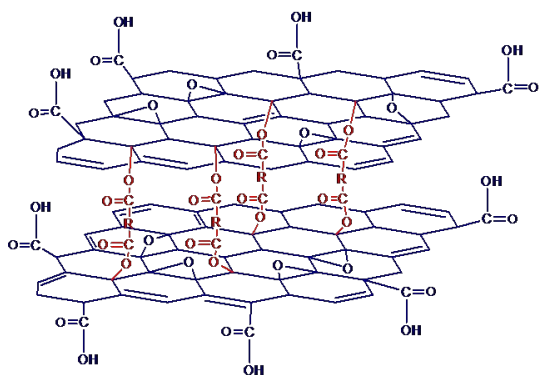

Scheme 1 Crosslinking mechanism with dicarboxylic acid (HOOC-R-COOH) as crosslinkers.

The FTIR spectra of GO membranes show that, for the pristine GO membrane, the broad peak appearing at 3214 cm^{-1} is assigned as stretching vibrations of O−H groups on GO (Fig. 2a).

The peaks at 1630 cm^{-1} and 1720 cm^{-1} are typical absorptions of carbonyl and carboxyl groups.[32] 1380 cm^{-1} is the vibration of C−O on GO, and the peak at 1049 cm^{-1} is due to the C−O−C (−epoxy−) vibration. [33] After crosslinking, a new stretching peak ascribed to C-H in the crosslinked dicarboxylic acid appears, and the intensities of C=O (1720 cm^{-1}) and C−O (1300-1050 cm^{-1}) peaks increase. The GO membrane crosslinked by HA exhibits the strongest IR feature absorption.

The X-ray photoelectron spectroscopy (XPS) results of the membrane surface layer are given in Fig. 2 b and c. In the curve fitting of C1s spectra of the pristine GO membrane (Fig. 2b), the binding energy of 284.8 eV is ascribed to C=C and C−C, and 285.8 eV is assigned to C−OH. 286.9 eV corresponds to C (epoxy), and 288.4 eV is from C=O. The binding energy of 289.4 eV is due to C(O)O.[34, 35] After crosslinking (Fig. 2c), the intensity of C−OH reduces due to its reaction with the dicarboxylic acid. Fig. 3 shows the scanning electron microscope (SEM) images of the GO membranes. The GO membranes possess a wrinkled surface topography and a well-layered lamellar structure. The membrane thickness was about 17.1 μm.
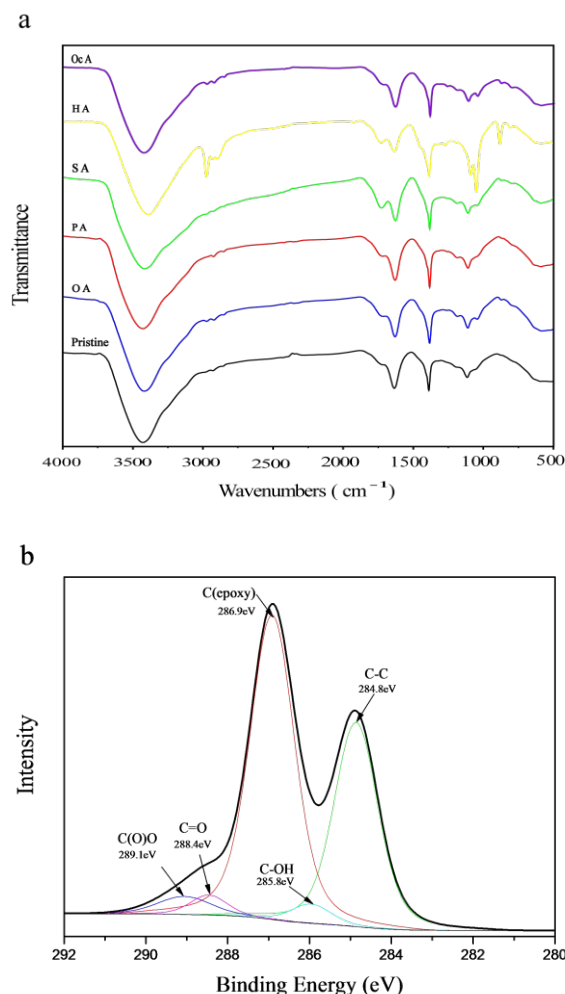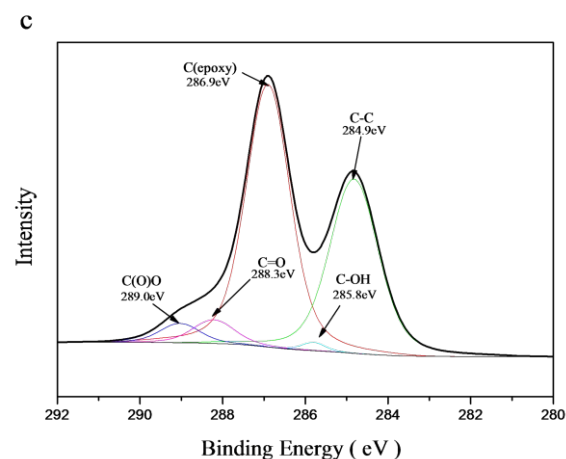
Fig. 2 FTIR and XPS spectra of GO membranes. (a) FTIR spectra (b) Curve fitting of XPS C1s spectra of pristine GO membrane. (c) Curve fitting of XPS C1s spectra of HA crosslinked GO
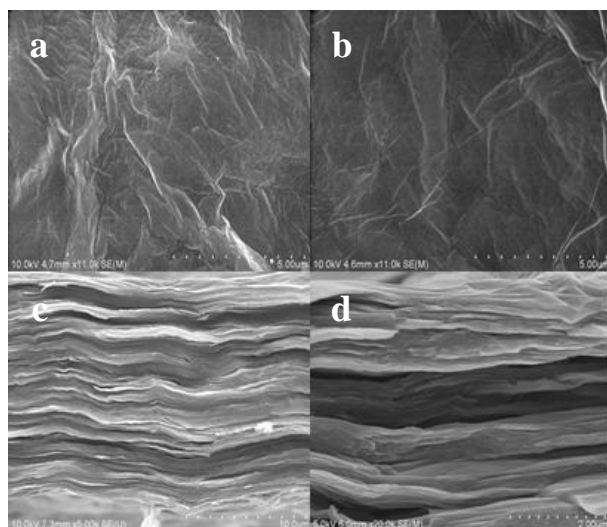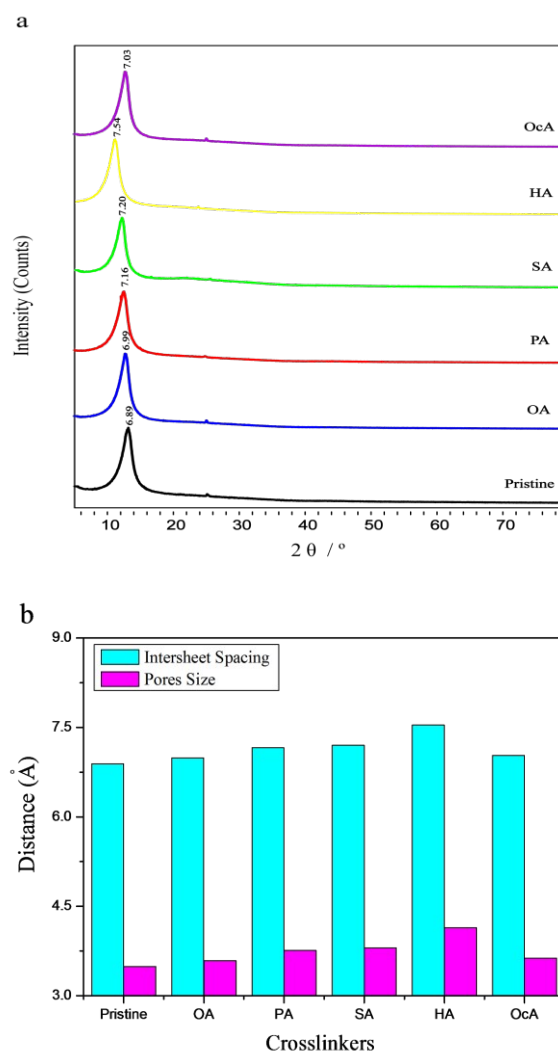5 membrane.

Fig. 3 SEM images of GO membrane. (a) Surface morphology of pristine GO membrane. (b) Surface morphology of crosslinked
10 GO membrane. (c) Cross section of pristine GO membrane. (d) Cross section of crosslinked GO membrane.

The laminated structure of GO membranes was further investigated using XRD. As shown in Fig. 4 a, the diffraction
15 peak of the pristine GO membrane is located at $2\theta=10.8$, corresponding to an intersheet spacing of 6.89 Å. For the GO membranes using OA, PA, SA and HA as crosslinkers, with the increase in molecular chain length, the diffraction peak moves to a lower angle, and the intersheet spacing rises from 6.99 Å to
20 7.54 Å due to intercalation effects (Fig. 4 b). Taking into account the thickness of single-layer of graphene sheet (3.40 Å),[10] the pores size (i.e. void spacing, which equals the deference between the intersheet spacing of GO and the thickness of graphene sheet) between adjacent GO sheets can be obtained (3.49~4.14 Å, Fig.
25 4b). It was noticed that, probably due to the strong hydrophobility

of OcA, its molecule chain may shrink upon contacting with the hydrophilic GO and hydrochloric acid, resulting in an abnormal small intersheet spacing.

Fig. 4c gives the mechanical properties of the as-obtained GO
30 membranes. With the rising molecular length of the crosslinkers, the elastic moduli of the GO membrane increase dramatically except for OcA. The HA crosslinked GO membrane displays the highest elastic modulus and attains to 4.6895 GPa (about 15.6 times that of the pristine one), whereas the OcA crosslinked
35 membrane shows small elastic modulus probably due to its low degree of esterification. It seems that there is an optimum chain length of crosslinkers: if the molecular chain is too short, the two carboxyl groups of the crosslinkers may not covalently link the hydroxyl groups on the adjacent GO sheets simultaneously; if the
40 molecular chain is too long, its hydrophility and affinity to GO sheets is low, resulting in a low degree of esterification.
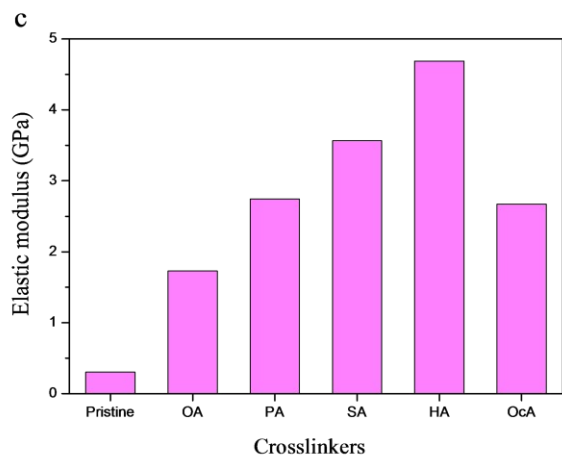
Fig. 4 (a) XRD patterns of GO membranes (b) Intersheet spacing and pores size of GO membranes (c) Elastic modulus of GO membranes.

5

A serious of penetration experiments were conducted with a U-type tube, which is divided by a GO membrane into two compartments. For penetration of single solution, the feed compartment contained KCl, $K_4Fe(CN)_6$ or glycerol aqueous
10 solution, while the permeate compartment contained pure water. The cations and anions move through the membrane in stoichiometric to preserve charge neutrality. There was no change in the liquid levels after penetration. The concentration change in the permeate compartment reflects the permeation flux. Fig. 5 (a)
15 shows that, for OA, PA and HA crosslinked GO membranes, the KCl concentrations in the permeate increase with time in a linear manner. For HA crosslinked membrane, with the rising KCl feed concentrations (0.050, 0.10 and 0.20 mol L^{-1}), the permeation fluxes of KCl increases from 0.025 to 0.028 and 0.049 mol h^{-1} m^{-2}
20 due to the increased driving force. Fig. 5 (b) reveals the effects of various crosslinkers on the permeation fluxes of KCl and K_4 [Fe(CN)$_6$]. With the increase in alkyl length of dicarboxylic acids, the permeation fluxes rise slightly. For the same membrane, the permeation flux of KCl is larger than that of
25 $K_4[Fe(CN)_6]$ because of the smaller radius of Cl$^-$ anion (Table 1). The OcA crosslinked GO membrane displays damage after a period of permeation due to the low degree of esterification, resulting in an abnormal large penetration flux. No glycerol was detected in the permeate compartment during 72 h for all of the
30 GO membranes.

For the penetration of mixed solution, the feed compartment contained the mixed MgCl$_2$, KCl, CaCl$_2$ and NiCl$_2$ aqueous solutions (each salt having the same concentration: 0.050, 0.10 or 0.20 mol L^{-1}). Fig.5 (c) shows the permeation fluxes of various
35 metal chlorides through the crosslinked and pristine GO membranes. It can be seen that, the permeation fluxes show a trend of K$^+$ > Ca^{2+} > Ni^{2+} > Mg^{2+}, following approximately the order of ions diffusivity or the converse order of ions radii (Table 1). At the same concentration, the permeation fluxes of HA
40 crosslinked membrane are higher than that of pristine membrane due to the enlarged intersheet spacing. At the salts concentration of 0.10 and 0.20 mol L^{-1}, the respective selectivity of K$^+$/Mg^{2+} are
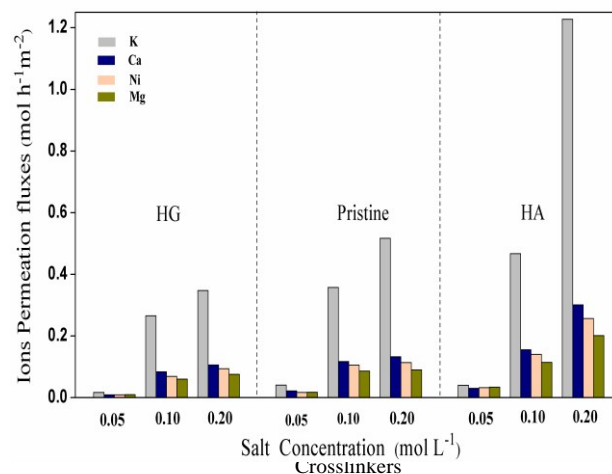
4.19 and 6.11 for HA crosslinked membrane, and 4.16 and 5.76 for pristine membrane, confirming the size selectivity of GO
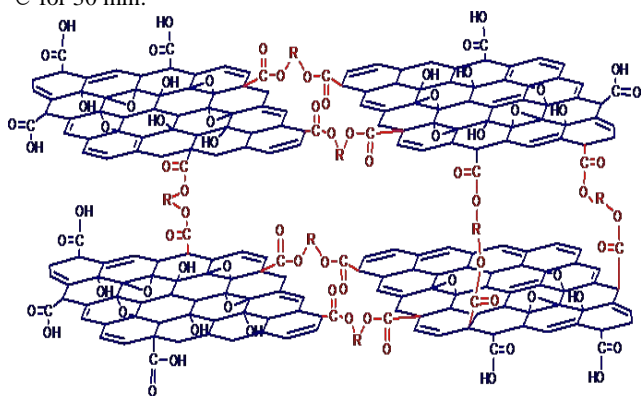45 membranes.
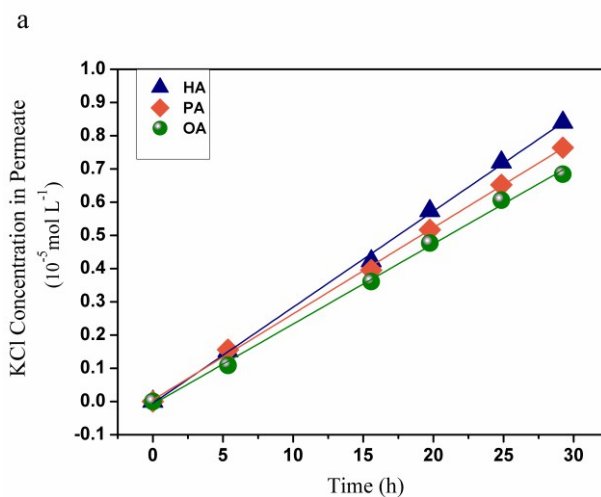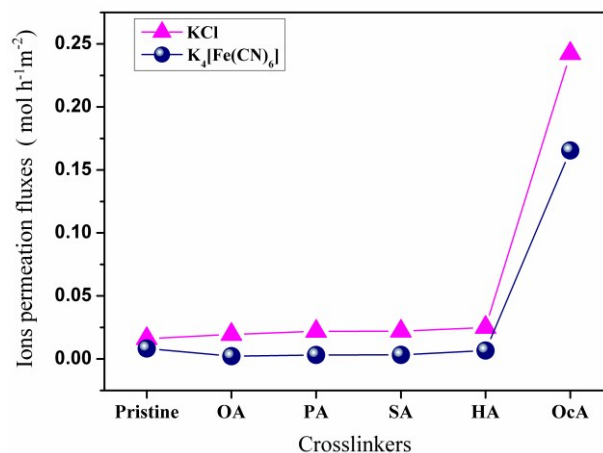
50

Fig. 5 Ion-penetration of GO membranes. (a) Changes of KCl
5 concentration in the permeate with time (0.050 mol L^{-1} of feed
solution). (b) Effects of various crosslinkers on the permeation
fluxes of single inorganic salts (0.050 mol L^{-1} of feed solution). (c)
Permeation fluxes of mixed salts solution through the crosslinked
and pristine GO membranes.

10

Table 1 Radius and diffusivity of hydrated metal ions.

Hydrate metal ions	Radius (Å)[36]	Ions diffusivity in water (10^{-10} m^2 s^{-1}, 25℃)[37]
K$^+$	3.31	19.57
Ca^{2+}	4.12	7.92
Ni^{2+}	4.04	7.05
Mg^{2+}	4.28	7.06
Cl$^-$	3.32	20.3
[Fe(CN)$_6$]$^{4-}$	4.22	7.35

15

20

Effects of diols or polyols

Diols or polyols, such as ethylene glycol (EG), 1,2-propylene
glycol (PG), butylene glycol (BG), 1, 6-hexylene glycol (HG),
neopentyl glycol (NPG), glycerol (GL) and pentaerythritol
25 (PER), were used to crosslink the carboxyl groups on the edges of
GO sheets (Scheme 2). The reactions were conducted at 0.01 mol
L^{-1} of diols or polyols, 9.60 mol L^{-1} of hydrochloric acid, and 80
℃ for 30 min.

30

Scheme 2 Crosslinking mechanism with diols (HO-R-OH))
as crosslinkers.

The FTIR spectra (Fig. 6) shows that, in contrast to the
35 pristine GO membrane, the stretching vibrations of O-H (3214
cm^{-1}) and C-O (1300-1050 cm^{-1}) of crosslinked GO membranes
become stronger, and a new C-H vibration originated from the
crosslinkers appears. The HG crosslinked GO membrane exhibits
the strongest IR feature absorption. Table 2 shows the effects of
40 diols or polyols on the intersheet spacing, elastic moduli and
permeation fluxes of inorganic salts. The intersheet spacing of the
pristine GO membrane is 6.89 Å, and it increases to 7.58 Å for
the EG crosslinked GO membrane. Then, with the increased alkyl

length of diols (EG, BG, HG), the intersheet spacing does not
45 exhibit obvious change because the diols react with the carboxyl
on the GO edge, and the intercalation effects are not apparent.
For NPG, GL and PER, their main chain is the same while the
substituents are various, and the order of intersheet spacing is as
follows: NPG (7.65 Å) > PER (7.63 Å) > glycerol (7.61Å). It
50 seems that, the hydrophobic substituent (-CH$_3$) tends to enlarge
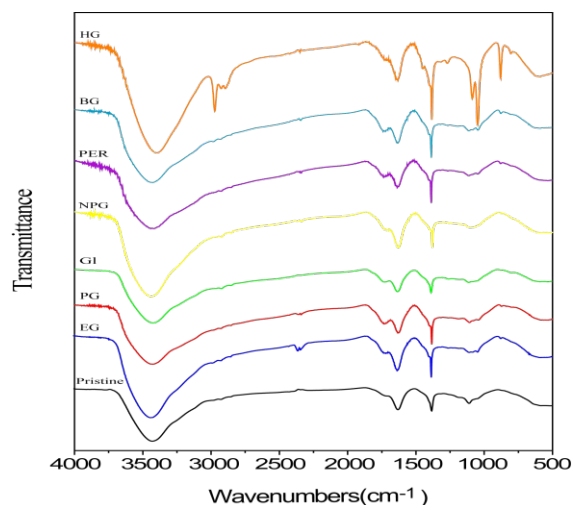the intersheet spacing. The same trend applies to EG and PG.

55 **Fig. 6** FTIR spectra of GO membranes cross-linked by di- or
polyol.

60

65

70

75

80

Table 2 Effects of diols or polyols on the intersheet spacing,
elastic moduli and permeation fluxes

Crosslinkers	Formula	Intersheet spacing /Å	Pore size /Å	Elastic moduli /GPa	Permeation fluxes (10⁻² mol m⁻² h⁻¹)	
					KCl	K₄Fe(CN)₆
Pristine GO		6.89	3.49	0.0345	1.611	0.424
EG	HO—H₂C—CH₂—OH	7.58	4.18	1.4474	1.761	0.570
PG	HO—H₂C—CH—OH, CH₃	7.63	4.23	2.4333	1.817	0.613
Gl	HO—H₂C—CH—CH₂—OH, OH	7.61	4.21	3.3778	2.636	0.640
NPG	HO—CH₂—C(CH₃)(CH₃)—CH₂—OH	7.65	4.25	2.2041	1.699	0.395
PER	HO—CH₂—C(CH₂OH)(CH₂OH)—CH₂—OH	7.63	4.23	2.0018	2.972	0.679
BG	HO—CH₂—CH₂—CH₂—CH₂—OH	7.63	4.23	2.5000	2.295	0.569
HG	HO—CH₂—CH₂—CH₂—CH₂—CH₂—CH₂—OH	7.59	4.19	3.4877	2.416	0.477

For straight-chain diols (EG, BG, HG), with the rising alkyl chain length, the elastic moduli of the crosslinked membranes increase, and the HG crosslinked one reaches 3.4877 GPa, about 10 times that of the pristine GO membrane. It was noticed that the elastic moduli of di- or polyol crosslinked membranes are usually lower than that of the dicarboxylic acids crosslinked ones. The reason is that the dicarboxylic acids crosslink the hydroxyl groups on the GO basal planes, and the interaction between GO sheets is greatly enhanced; whereas the di- or polyols crosslink with the carboxyl on the GO edges and their effects on the interaction between GO sheets are not so significant. For NPG, GL and PER crosslinked membranes, the permeation fluxes of the inorganic salts display the trend of PER > GL > NPG, indicating that the hydrophilic substituent (-OH) is beneficial for the penetration of hydrous ions. Fig.5(c) shows that, for the HG crosslinked GO membranes, the permeation fluxes of ions increase with the salts concentration. At the salt concentration of 0.20 mol L⁻¹, the K^+/Mg^{2+} selectivity reaches 4.62.

Mechanism and model

According to previous reports, [10, 11] the oxygen-containing functional groups on GO tend to cluster together, leaving other nonoxidized regions to form a two-dimensional network of nanocapillaries. These nanocapillaries provide high capillary pressures facilitating the low-friction flow of water, whereas the water molecules within the oxidized regions exhibit poor mobility due to the hydrogen-bonds interaction with the functional groups. When the pristine GO membrane is immersed in an aqueous solution, hydration increased the GO spacing to ~0.9 nm.[39] When the spacing becomes sufficiently large, the nanocapillaries allow the permeation of hydrated ions. For pristine GO membranes, the oxygen-containing functional groups can coordinate with a variety of metal ions and results in selective penetration properties of GO membranes, which cannot be explained solely by ionic-radius-based theories.[38] Nevertheless, our experimental results demonstrate that the crosslinked GO membranes display size selectivity to hydrated ions. The reason is that the hydroxyl groups on the surface (or the carboxyl on the edges) of GO sheets are esterified by dicarboxylic acid (or diol, polyol), leading to a decreased coordination ability of GO sheets with metal ions. Therefore, sieving effect plays a crucial role in the separate of ions by the crosslinked GO membranes.

Fig. 7(a) presents the schematic diagram of the cross-section of GO membranes. For simplification, presuming that the GO sheets with a typical size of L display a brick-wall stacking, and the thickness of the GO membrane is h, and the intersheet spacing is d (in this paper, L≈1 μm, d ≈ 1 nm, h ≈ 17.1 μm), the number of GO layers is h/d = $1.7×10^4$. The penetration length of ions through GO membrane is expressed as

$$L_{eff} = \frac{h}{d}\left(\frac{L}{2}+d\right) \approx \frac{hL}{2d} \approx 8.5 mm \qquad (1)$$

Obviously, the bottleneck in this process is the passage between GO sheets. The schematic of the GO membrane surface is given in Fig. 7(b). Provided that the spacing of GO sheets is d, the surface porosity for ions diffusion is written as

$$\varepsilon = \frac{(L+d)^2 - L^2}{(L+d)^2} = \frac{d^2+2dL}{(L+d)^2} \approx \frac{2d}{L} = 0.002 \qquad (2)$$

In our experiments, the GO membrane area A=1.3273 cm², and the effective pores area of the GO membrane is A_{eff} = Aε = 2.6546 ×10⁻³ cm². Eqs (1) and (2) are modified equations of Nair's.[10] Provided that the effective diffusion coefficient is D_{eff}, the ions permeation flux J（mol h⁻¹ m⁻²) is written as,

$$J = \frac{Q}{A_{eff}} = D_{eff}\frac{\Delta C}{L_{eff}} \qquad (3)$$

Apparently, D_{eff} includes the effects of the interaction between ions and the GO membranes. Under the same crosslinking conditions, A_{eff}, L_{eff} and ΔC are the same, and the permeation flux is proportional to D_{eff}. A typical diffusion coefficient of ions in water is 10^{-10} m^2 s^{-1}, and the initial concentration difference in our experiments ΔC equals 0.050, 0.10 and 0.20 mol L^{-1}, respectively. Then, from Eqs.(3), J is found to be 2.12×10^{-9}, 4.24×10^{-9} and 8.48×10^{-9} mol h^{-1} m^{-2}, which are about 7 orders of magnitude lower than the measured values (10^{-2} mol h^{-1} m^{-2}), indicating that the ions penetration is accelerated by capillary effects. This is in consistent with Nair's report.[10] It is noticed that, compared with the dicarboxylic acids crosslinked membranes, the permeation fluxes and selectivity of di- or polyols crosslinked are relatively lower (Fig. 5c, Table 2), indicating that the crosslinking sites have important effects on the diffusion path and then the permeation performance of GO membranes.
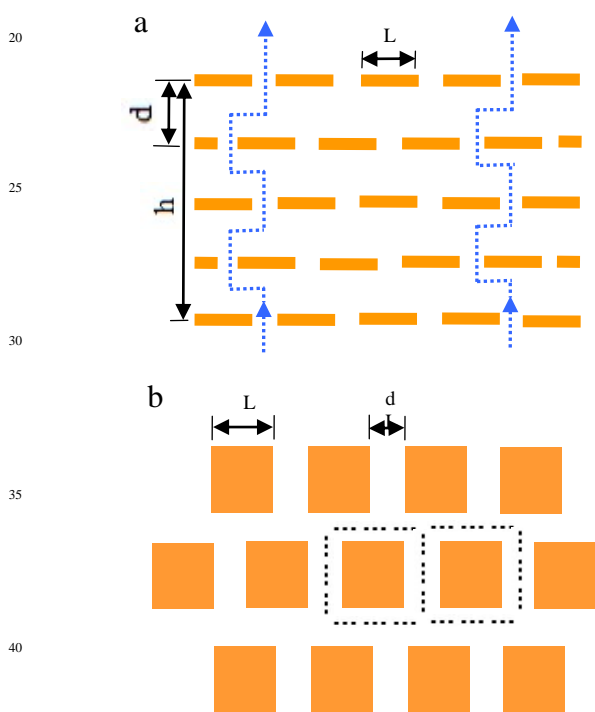

Fig. 7 Schematic of the GO membrane. (a) Cross-section of the GO membrane. (b) Surface of the GO membrane.

Conclusions

GO membranes were covalently crosslinked by esterification reactions. For dicarboxylic acids crosslinked membranes, with the rising molecular length, the intersheet spacing, elastic moduli and permeation fluxes generally increase. For diols or polyols, the hydrophobic substituents enlarge the intersheet spacing while the hydrophilic substituents favor the penetration of hydrous ions. The crosslinking sites have important effects on the structure and permeation performance of GO membranes. The crosslinked GO membranes display excellent size-selectivity to hydrous ions, indicating its great potential in ions separation.

Notes and references

1. W. W. Ho and K. K. Sirkar, *Membrane handbook*, Springer, 1992.
2. J. Luo, L. J. Cote, V. C. Tung, A. T. L. Tan, P. E. Goins, J. Wu and J. Huang, *J. Am. Chem.Soc.*, 2010, **132**, 17667-17669.
3. X. Li, X. Wang, L. Zhang, S. Lee and H. Dai, *Science*, 2008, **319**, 1229-1232.
4. H. W. Kim, H. W. Yoon, S.-M. Yoon, B. M. Yoo, B. K. Ahn, Y. H. Cho, H. J. Shin, H. Yang, U. Paik, S. Kwon, J.-Y. Choi and H. B. Park, *Science*, 2013, **342**, 91-95.
5. H. Li, Z. Song, X. Zhang, Y. Huang, S. Li, Y. Mao, H. J. Ploehn, Y. Bao and M. Yu, *Science*, 2013, **342**, 95-98.
6. C. Chen, Q.-H. Yang, Y. Yang, W. Lv, Y. Wen, P.-X. Hou, M. Wang and H.-M. Cheng, *Adv. Mater.*, 2009, **21**, 3007-3011.
7. G. Szalóki, G. Sevez, J. Berthet, J.-L. Pozzo and S. Delbaere, *J. Am. Chem.Soc.*, 2014, 136, 13510–13513.
8. K. S. Kim, Y. Zhao, H. Jang, S. Y. Lee, J. M. Kim, K.S. Kim, J.-H. Ahn, P. Kim, J.-Y. Choi and B. H. Hong, *Nature*, 2009, 457, 706-710.
9. J. Kim, L. J. Cote and J. Huang, *Acc. Chem. Res.*, 2012, **45**, 1356-1364.
10. R. R. Nair, H. A. Wu, P. N. Jayaram, I. V. Grigorieva and A. K. Geim, *Science*, 2012, **335**, 442-444.
11. F. Guo, G. Silverberg, S. Bowers, S.-P. Kim, D. Datta, V. Shenoy and R. H. Hurt, *Environ. Sci.Technol.*, 2012, **46**, 7717-7724.
12. Y.-H. Yang, L. Bolling, M. A. Priolo and J. C. Grunlan, *Adv. Mater.*, 2013, **25**, 503-508.
13. R. Zangi and A. E. Mark, *Phys. Review Lett.*, 2003, **91**, 025502(1-4).
14. B. Mi, *Science*, 2014, **343**, 740.
15. K. Goh, L. Setiawanc, Li Wei, R. Si, A. G. Fane, R. Wang and Chen.*J. Membr. Sci.*2015, **15**, 244–253.
16. J. Shen, G. Liu, K. Huang, W. Jin, K. Lee and N. Xu. *Angew. Chem.*, DOI: 10.1002/ange.201409563
17. H. W. Kim, B. M. Yoo, J. S. Park, K. L. Gleason, B. D. Freeman and H. B. Park. *Chem. Commun.*, 2014,**50**, 13563-13566
18. O. C. Compton and S. T. Nguyen, *Small*, 2010, **6**, 711-723.
19. J. Zou and F. Kim, *ACS Nano*, 2012, **6**, 10606-10613.
20. Q. Cheng, M. Wu, M. Li, L. Jiang and Z. Tang, *Angew. Chem.*, 2013, **125**, 3838-3843.
21. S. Park, K.-S. Lee, G. Bozoklu, W. Cai, S. T. Nguyen and R. S. Ruoff, *ACS Nano*, 2008, **2**, 572-578.
22. Z. An, O. C. Compton, K. W. Putz, L. C. Brinson and S. T. Nguyen, *Adv.Mater.*, 2011, **23**, 3842-3846.
23. S. Park, D. A. Dikin, S. T. Nguyen and R. S. Ruoff, *J. Phys. Chem. C*, 2009, **113**, 15801-15804.
24. L. Chen, L. Huang, J. Zhu, *Chem. Commun.*, 2014, DOI: 10.1039/C4CC07558G.
25. Y. Tian, Y. Cao, Y. Wang, W. Yang and J. Feng, *Adv.Mater.*, 2013, **25**, 2980-2983.
26. Y. Liu, J. Zhou, E. Zhu, J. Tang, X. Liu and W. Tang.*Carbon*, 2015,82, 264–272.
27. Y. Gao, L.-Q. Liu, S.-Z. Zu, K. Peng, D. Zhou, B.-H. Han and Z. Zhang, *ACS Nano*, 2011, **5**, 2134-2141.
28. P. Sun, F. Zheng, K. Wang,1 M. Zhong, D. Wu and H. Zhu. *Scientific Reports,* 2014 (DOI: 10.1038/srep06798)
29. J.He, J. Zhou, X. Lu and B.Corry. *ACS Nano*, 2013,**7**, 10148–10157.
30. Y. Zhu, S. Murali, W. Cai, X. Li, J. W. Suk, J. R. Potts and R. S. Ruoff, *Adv.Mater.*, 2010, **22**, 3906-3924.
31. D. D. Kulkarni, I. Choi, S. S. Singamaneni and V. V. Tsukruk, *ACS Nano*, 2010, **4**, 4667-4676.
32. G. Wang, B. Wang, J. Park, J. Yang, X. Shen and J. Yao, *Carbon*, 2009, **47**, 68-72.

33. D. W. Lee, L. De Los Santos V, J. W. Seo, L. L. Felix, A. Bustamante D, J. M. Cole and C. H. W. Barnes, *J. Phys. Chem. B*, 2010, **114**, 5723-5728.

34. A. R. Kumarasinghe, L. Samaranayake, F. Bondino, E. Magnano, N. Kottegoda, E. Carlino, U. N. Ratnayake, A. A. P. de Alwis, V. Karunaratne and G. A. J. Amaratunga, *J. Phys. Chem. C*, 2013, **117**, 9507-9519.

35. L. Chen, Z. Xu, J. Li, Y. Li, M. Shan, C. Wang, Z. Wang, Q. Guo, L. Liu, G. Chen and X. Qian, *J.Mater. Chem.*, 2012, **22**, 13460-13463.

36. E.R. Nightingale Jr., *J. Phys. Chem.* 1959,63, 1381–1387.

37. Henry V. K. (Ed.) CRC handbook of thermophysical and thermochemical data. CRC press Inc. Boca Raton, 1994

38. R. K. Joshi, P. Carbone, F. C. Wang, V. G. Kravets, Y. Su, I. V. Grigorieva, H. A. Wu, A. K. Geim and R. R. Nair, *Science*, 2014, **343**, 752-754.

39. P. Sun, M. Zhu, K. Wang, M. Zhong, J. Wei, D. Wu, Z. Xu and H. Zhu, *ACS Nano*, 2012, **7**, 428-437.

.

.